Available online at www.sciencedirect.com

jmr&t Journal of Materials Research and Technology

journal homepage: www.elsevier.com/locate/jmrt

Original Article

Aluminium dross/soda lime glass waste-derived high-quality glass foam

Ahmed A.M. El-Amir [a,*], Mohammed A.A. Attia [b], M. Newishy [a], Thomas Fend [c], Emad M.M. Ewais [a]

[a] Refractory and Ceramic Materials Dept., Central Metallurgical Research and Development Institute, Cairo, Egypt
[b] Mechanical Engineering Dept., Faculty of Engineering, Helwan University, Cairo, Egypt
[c] German Aerospace Center (DLR), Cologne, Germany

ARTICLE INFO

Article history:
Received 2 July 2021
Accepted 19 October 2021
Available online 28 October 2021

Keywords:
Cellular glass foams
Recycled soda-lime glass waste
Aluminium dross
3-D cellular-like structure

ABSTRACT

This work introduces for the first time the use of waste aluminium dross obtained from the aluminium industry as a foaming agent to produce sustainable foam glasses from soda-lime glass powders derived from the lapping machine. The resulting foam briquettes (8x8x8 cm^3) have a crack-free, 3-D cellular structure with closed pores whose geometries varied between elliptical-, pentagonal-, and hexagonal-shaped constructions. These glass foams demonstrate a lightweight (≥0.28 g/cm^3), high CCS (≤12 MPa), low thermal conductivity (0.11–0.21 W/m-K), and contain more than ~ 85 vol.% gas bubbles enclosed between 15 vol.% impervious glass walls. These properties are in line with the requirements of the international standard for commercial glass foams, revealing their strong capability to be used in potential applications in sustainable buildings and energy efficiency in the industry.

1. Introduction

Recycling of industrial wastes and by-products is nowadays a priority and has recently attracted an increasing area of interest due to depletion of natural resources and accumulation of massive amounts of solid wastes, which subsequently leads to a disposal crisis and affects negatively human health, air, and water quality. Among these solid wastes, millions of tons of glass scraps are annually produced. These glass wastes are polluted with a high proportion of fine organic substances as well as metallic and non-metallic crumbs. The cost of removal of these organic and inorganic inclusions is fairly high. Therefore, in many cases, the production of articles using glass scraps is a low-profit operation. Consequently, the amounts of accumulated glass wastes are gradually increasing in landfills due to the limitations of glass recycling and the growing demand for the glass industry. For example, in UE, about 25.8 MMT solid glass wastes were generated in 2015 from which about ~11 MMT (42.6%) were recycled and 14.8 MMT (57.4%) were landfilled [1], while in the USA 3 MMT (26%) were recycled from 11.5 MMT to 8.5 MMT (74%) were landfilled [2]. The global quantity of glass wastes produced in 2018 was approximately 130 MMT; 48% of these wastes (~62.4

* Corresponding author.
E-mail address: elamirahmed.ahmed@gmail.com (A.A.M. El-Amir).
https://doi.org/10.1016/j.jmrt.2021.10.085

Table 1 – Comparison between physico-mechanical properties of glass foams prepared in previous and current works.

Glass waste	Foaming agent, wt.%	additives	Foaming temp., °C	Holding time, min	BD, g/cm^3	CCS, MPa	AP, Vol.%	Reference
Bottle glass	SiC	Fly ash	950	20	0.267	0.982	81.55	[11]
CRT panel& SCS glasses	SiC, dol., Cal. & marble dross	Fly ash	850	–	0.25–0.39	1.4–2.6	–	[12]
Glass scrap	Graphite (2wt.%)		880	10	0.677	–	–	[13]
Soda-lime glass	Dol.	clay	1000–1075		0.76–1.4	0.42–2.3	33–62%	[14]
Soda-lime glass	AlN (2.5–7.5 wt.%)	–	850–950	30	≤0.5	0.65–2.48	≤94	previous work [15]
Soda-lime glass	Aluminium dross (2.5–7.5 wt.%)		900–1000	30	≥0.28	≤12	≤91	Current work

CRT: cathode ray tube; SCS: sodium-calcium-silicate; Dol.: dolomite; Cal.: calcite; AP: apparent porosity; BD: bulk density.

MMT) were generated from hollow glass containers; 42% (~54.6 MMT) were derived from the flat glass products (car glass, window and construction glasses); 5% (~6.5 MMT) are accounted for by tableware; and 5% (~6.5 MMT) were produced from other glass products [3,4]. About 32% of the container glasses and 11% of the flat glasses are typically recycled and the rest of these urban solid wastes is progressively accumulated in the landfills, causing severe environmental problems. Dealing with such massive amounts of glass scrap is a serious problem that must be solved.

Luckily, the incorporation of glass waste in the production of cellular glass foam has recently attracted much interest in the recycling concept and provided an important way to recycle these glass scraps. Foamed glass is an exceptional material that is widely used for various applications such as filters for hot gases and molten metals, refractory linings, catalyst support, and building materials [5] due to their superior combination of characteristics such as nontoxicity, chemical inertness, lightweight (>0.5 g/cm^3), high porosity content (<60 vol.%) [6], moderate compressive strength values (0.4–6 MPa) [7], fire-resistance, water-resistance, high thermal insulation (~0.1 Wm^{-1}K^{-1}), bacterial resistance, ease of handling, cutting, and drilling, as well as its high-affinity to concrete [8,9].

Generally, glass foams are typically synthesized via foaming glass matrices by a pore-forming agent such as carbon, silicon carbide, carbonates, and sulfates near the glass softening temperature undergoing viscous flow sintering [10]. Glass foams have produced from a number of glass wastes using various pore-forming agents; the characteristics of these foam glasses were summed up in Table 1. J. Bai et al. have utilized the bottle glass wase, fly ash together with SiC foaming agent to synthesize glass foams at 950 °C for 20 min. The resulting glass foams had a closed-pore structure with 81.55 vol.% porosity, 267.2 kg/m^3 bulk density, and 0.9829 MPa cold crushing strength [11]. In another work, the production of glass foams from two types of glass wastes (cathode ray tube panel glass waste and sodium-calcium-silicate sheet glass cullet), fly ash, and various pore-forming agents (commercial and waste SiC, dolomite, calcite, and marble dross) was studied; 2 wt.% of dolomite or calcite was quite enough to get glass foams featuring interesting characteristics (1.4–1.6 MPa CCS and 0.36–0.39 g cm^{-3} bulk density) starting from the glass cullet at 850 °C. The addition of 1 wt.% SiC to glass cullet has resulted in the production of glass foams with 2.6 MPa CCS and 0.25 g cm^{-3} bulk density [12]. The glass foams produced from glass mixture with 2 wt.% graphite pore-forming agent at 880 °C for 10 min achieved 214 μm an average aperture, and 0.677 g/cm^3 bulk density [13]. In another work, the effect of clay additives on the foaming and mechanical characteristics of glass foams prepared from soda-lime glass waste and dolomite as a pore-forming agent was duly studied [14]; the resulting foams demonstrated 0.42–2.3 MPa compressive strength, 0.76–1.4 g/cm^3 bulk density, and 33–62% apparent porosity in the temperature range 1000–1075 °C. Our research group has recently paid more attention to the utilization of landfilled glass cullet in the production of glass foams, contributing to saving the environment and providing an added value to these wastes. During the last years, Ewais et al. have synthesized glass foam blocks with 0.65–2.48 MPa cold crushing strength, ≤ 0.5 g cm^{-3} bulk density, and 0.09–0.106 Wm-1K-1 thermal conductivity starting from soda-lime glass waste together with 2.5–7.5 wt.% nano AlN foaming agent [15].

In this study, the possibility of recycling a high percentage of up to 100% of the industrial residues in the production of high-quality structural foams was successfully introduced. This work added value for two types of industrial wastes where it presented for the first time utilization of aluminium dross waste obtained from the aluminium industry as a foaming agent for the production of sustainable foam glasses from the soda-lime glass powders derived from the lapping machine. The lapping machine is the instrument that is used to grind, polish and prepare the surface of the glass after the diamond tool. Aluminium slag was used as a foaming agent in this study because it contains a high proportion of aluminium nitride (15–30 wt.%), a well-known pore-forming agent [16–21]. What's more, the use of aluminium dross as a foaming agent increased the alumina content of the glass mixture and, consequently, improved the glass's resistance against melting. As a result, a higher sintering temperature was applied, and better crystallization conditions arose, which in turn led to the emergence of a glass foam with better characteristics compared to our previous work. The properties achieved by the glass foams produced in this work are in line with the requirements of the international standard for commercial glass foams, revealing their strong ability to be used in potential

applications in sustainable buildings and energy efficiency in the industry.

2. Materials and experimental procedure

2.1. Materials

The soda-lime glass waste resulting from the lapping machine was supplied by a municipal recycling company, Cairo, Egypt. A detailed elemental analysis of this industrial waste was presented in our previous article [15]; it composed mostly of SiO_2 (71.6 wt.%), Na_2O (13.5 wt.%), CaO (9 wt.%), MgO (3.87 wt.%) along with a small amount of Al_2O_3, Fe_2O_3, SO_3 and K_2O (about ~1.71 wt.%).

Aluminium dross was supplied by the Aluminium industry, Naga Hamad, Egypt. This slag was utilized as a foaming agent due to its high content of AlN (15–30 wt.%) that easily decomposes across the glass residue softening temperature range [16,19,22].

2.2. Experimental procedure

Typical experimental procedures were schematically outlined in Fig. 1. At first, the waste glass was crushed with a small crushing machine. The crushed glass was then ground in a planetary ball mill (weight ratio of glass:zirconia balls = 1:2) at 350 rpm for 90 min. The milled glass powder was subsequently sifted through a 50-mesh sieve. Three batch compositions (GF2.5–7.5) were manufactured from waste glass powders and aluminium dross foaming agents according to the nominal compositions displayed in Table 2. These batches were dry-blended in a planetary ball mill for 30 min, then dry-molded in stainless steel moulds (10x10x10 cm^3, interior surface coated with BN). The stainless-steel moulds were then placed in a muffle-furnace and heat-treated at 900–1000 °C with 5 °C/min heating rate and 30 min retention time at the

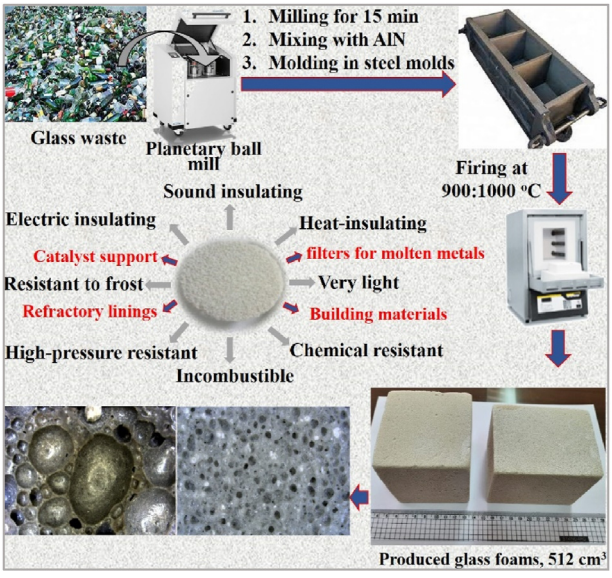

Fig. 1 – Schematic diagram of the typical experimental procedure.

Table 2 – Nominal composition of the designed batches.

Sample name	Chemical composition
GF2.5	2.5 wt.% alumina dross +97.5 wt.% soda lime glass waste
GF5	5 wt.% alumina dross +95 wt.% soda lime glass waste
GF7.5	7.5 wt.% alumina dross +92.5 wt.% soda lime glass waste

foaming temperature. After slow cooling to ambient temperature, demolding, cutting and finishing the sintered briquettes, 8x8x8 cm^3 glass foam bricks were obtained, as shown in schematic diagram in Fig. 1. The physical, mechanical and thermal characteristics of the resulting glass foams have been duly studied as a function of the foaming temperature and the pore-forming agent content. To avoid errors in the results, the measurement was carried out three times and the results were only accepted if the difference between the three values was less than 1.5%.

2.3. Characterization

The bulk density (BD) of the resulting cellular glass foams was measured by the simple equation, BD = W/V, where W: weight of glass foam and V: volume of glass foam. The relative density (RD) was estimated by RD = BD/2.52, where 2.52 g/cm^3 is the true density of the ground glass powder. From the relative density value, the apparent porosity (AP) was determined using the following equation, AP = 1-RD. The mineralogical composition of the synthesized glass foams was investigated using SHIMADZU X-ray diffraction machine (Model: XRD-7000, Japan, Cu kα radiation (λ = 1.5406 Å), 2-theta range from 5 to 70°). The microstructure and morphology of the prepared glass foams were examined by means of a field-emission scanning electron microscope (FESEM, Quanta FEG 250, Holland). The exact cellularity (number of pores per inch, PPI) was estimated by counting the number of pores intersected by a straight line (1″) on the obtained photomicrographs [23]. The compression resistance of the glass foam specimens was measured using Shimadzu testing machine at 1.3 mm/min displacement rate (Model: UH-F 1000 KN, Japan). Thermal conductivity, thermal diffusivity and specific heat capacity were measured by the Hot Desk machine (Model: 2500s, Sweden).

3. Results and discussion

One of the main pillars in the formation of high-quality glass foams is the heat-treatment process. Based on laboratory experiments, optimal foaming temperatures of soda-lime glass waste with aluminium dross were specified between 900 and 1000 °C. At these temperatures, soda-lime glass waste is suggested to form a highly viscous matrix, and aluminium dross decomposes producing gas bubbles that are entrapped in the viscous glass medium result in expanding the glass matrix and creating a cellular material. For better understanding the physical, mechanical, and thermal

characteristics of the resulting cellular materials, their respective microstructures were first analyzed.

3.1. *Microstucture*

FESEM photomicrographs of the resulting GF2.5-10 glass foams sintered at 900, 950, and 1000 °C were depicted in Figs. (2, 3, 4) respectively. The resulting glass foams demonstrated a 3D-cellular-like structure with crack-free and closed pores of irregular geometries that varied among pentagonal-, elliptical- and hexagonal-shaped structures. These pores were surrounded by struts of an inhomogeneous cell wall thickness. The variation in porosity (quantity, size, shape, and distribution of pores) of the produced foams was strongly influenced by the sintering temperature and the amount of pore-forming agent. The average aperture of the produced glass foams "GF2.5–7.5" sintered at 900–1000 °C were summed up in Table 3. The glass foams produced at low temperature, 900 °C, demonstrated thick pore walls and unevenly distributed pores with small diameters (0.045–0.27 mm), suggesting that the

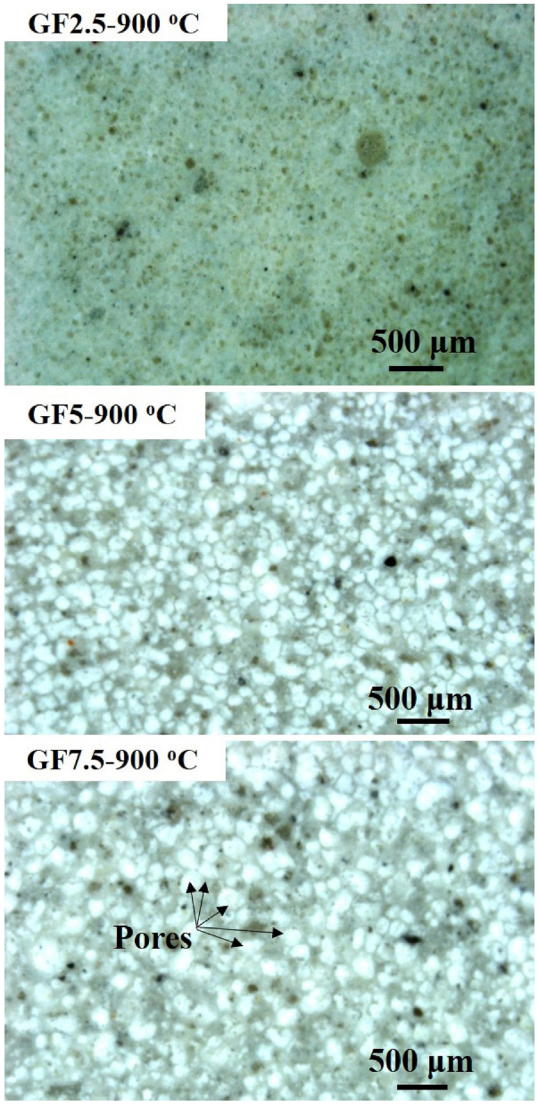

Fig. 2 – FESEM photomicrographs of the GF2.5–7.5 glass foams sintered at 900 °C.

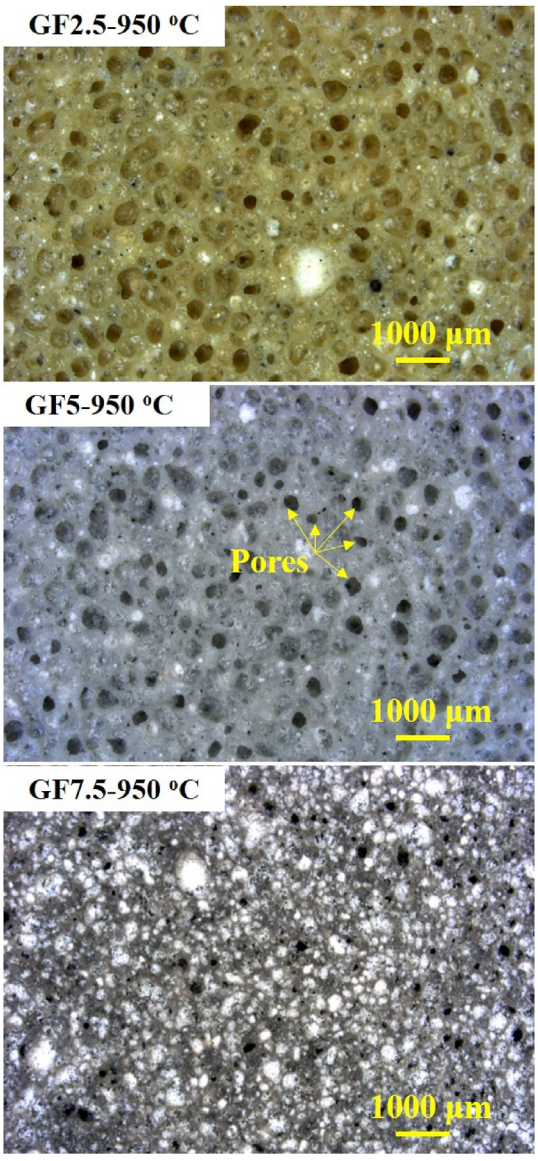

Fig. 3 – FESEM photomicrographs of the GF2.5–7.5 glass foams sintered at 950 °C.

average viscosity of the glass medium at 900 °C remains relatively high hindering further expansion of the foam. With the increase of sintering temperature up to 950 °C, the pore walls became thinner and the pore diameters became larger (0.227–0.739 mm) as well as more uniform. These observations suggest that the gas pressure in the pores and the surface energy of the melt reached equilibrium at this point. Beyond 950 °C, the viscosity of glass melt decreased significantly and the internal gas pressure in the pores reached a certain limit forcing the pores to considerably grow and the walls to thin, leading to gas escape and causing some voids to merge forming large and/or connected holes with an aperture size of 1.241–7.594 mm [13,24]. At the optimal foaming temperature, 950 °C, the average aperture and apparent porosity were about 477 ± 250 µm and 84.7%, respectively, when the aluminium dross content was 2.5 wt.%. Upon rising the content of aluminium dross to 5 wt.%, apparent porosity and average

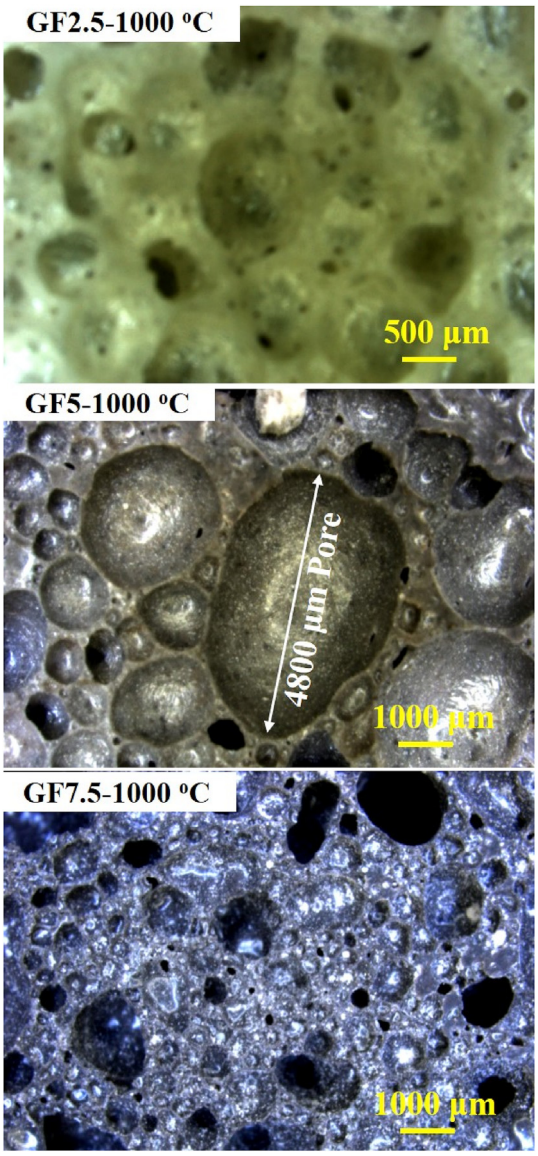

Fig. 4 – FESEM photomicrographs of the GF2.5–7.5 glass foams sintered at 1000 °C.

aperture increased respectively to 86.3% and 528 ± 200 μm. In contrast, the average aperture and porosity declined to 489 ± 250 μm and 81% when the aluminium dross quantity increased from 5 to 7.5 wt.%. This can be explained as follows: (1) when the dross content is low (2.5 wt.%), a small quantity of gases is evolved leading to small pore diameter and low apparent porosity (2) The porosity and average aperture size increased when the dross content increased to 5 wt.% due to releasing of more gas bubbles at high foaming agent content (3) Excessive amounts of dross beyond 5 wt.% caused accumulation of pores forming larger and/or connected pores leading to non-uniformity of pore size and bad foaming quality [25]. Such reduction in porosity and mean pore size when the foaming agent content is exceeded beyond a certain limit has been observed in several previous works [7,26,27] and it has been ascribed to the formation of gas in large quantities, the breakdown of struts, and the escape of gas bubbles. In light of these findings, the sintering temperature and the amount of pore-forming agents are the primary factors controlling the porosity variation in the final cellular foam products. The obtained results indicated that the produced foam glasses had the best quality when the foaming temperature was 950 °C and the aluminium dross content was 5 wt.%. Figure 5 showed the macrostructure and side views of the GF5 specimen (8x8x8 cm^3) foamed at 950 °C for 30 min.

Table 3 – Average aperture of the glass foams prepared at 900–1000 °C.

Sample name	Property		
	Mean pore size (μm)		
	900 °C	950 °C	1000 °C
GF2.5	65 ± 20	477 ± 250	2461 ± 600
GF5	160 ± 60	528 ± 200	3594 ± 3000
GF7.5	175 ± 95	489 ± 250	2141 ± 900

3.2. *Phase composition evolution*

Fig. 6 (a–c) displayed the powder XRD patterns of glass foam samples "GF2.5–7.5" fired at 900, 950, and 1000 °C, respectively. These cellular foams demonstrated amorphous XRD spectra with a wide halo in the 2θ range from 15 to 35° which is characteristic for the amorphous silica with silanol group (Si–OH) [28,29]. This indicates the amorphous structure of the glass foam samples fabricated in this work. Nevertheless, partially crystalline phases with very low-intensity diffraction peaks were observed in some of these glass foams such as diopside ($CaMg(SiO_3)_2$, at 2θ = 29.92 and 35.58°, #JCPDS#00-017-0318) and cristobalite (SiO_2, at 2θ = 21.72°, #JCPDS#01-082-0512). Diopside crystallization was reported in a number of glass foams produced from glass scraps and various foaming agents [12,14]. Cristobalite crystallization was also reported in

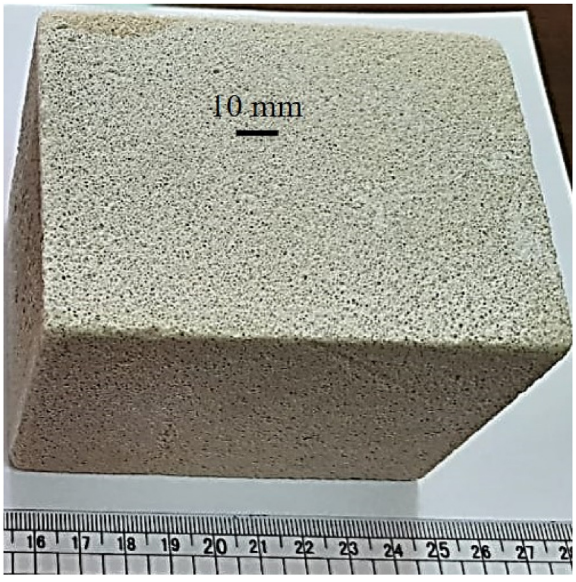

Fig. 5 – Macrostructure of the GF5 glass foam sintered at 950 °C for 30 min.

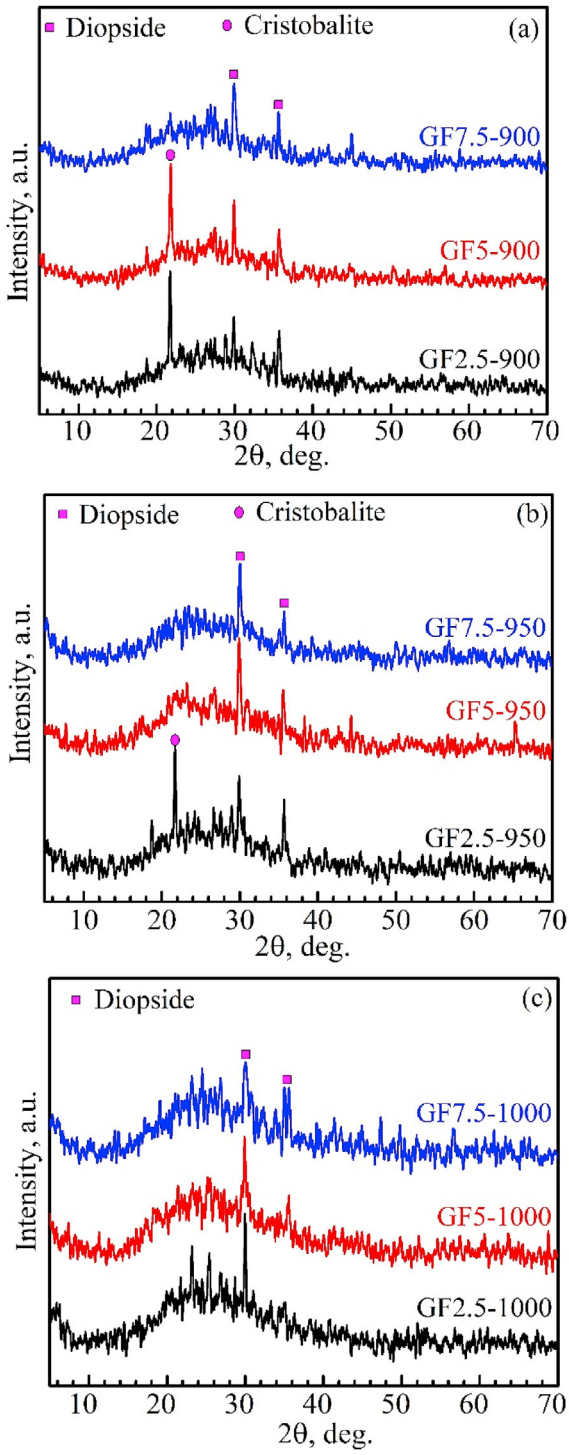

Fig. 6 – X-ray diffractograms of glass foams fired at (a) 900 °C, (b) 950 °C and (c) 1000 °C.

the studies performed on soda-lime glass wastes in references [7,11,30,31].

3.3. *Densification parameters*

Variations of bulk density, apparent porosity, and exact cellularity of the resulting glass foams "GF2.5–7.5" with sintering temperature and aluminium dross content were shown in Figs. 7, 8, 9, respectively. The results obtained showed good compatibility and a reciprocal relationship between density and apparent porosity, where the former increased when the latter decreased and vice versa. At 900 °C, the bulk density decreased, and otherwise the apparent porosity and cellularity increased straightforwardly as the amount of foaming agent increased from 2.5 to 7.5 wt.%. This can be easily explained in terms of the formation of larger quantities of gas bubbles as the amount of foaming agent increases [12]. At 900 °C, foamed samples were expanded clearly to 3–3.5 times compared to the green body, resulting in a foam with slightly high density (0.57 ± 0.04 g/cm^3), low porosity (82 ± 1 vol.%), small cellularity (36–82 PPI), and narrow pore size (45–270 μm). The volume expansion of the foamed samples at 900 °C is quite low, suggesting that the viscosity at this foaming temperature was still relatively high, preventing higher expansion of the samples. When the foaming temperature increased from 900 °C to 950 °C, analogous tendency (density decline and porosity enhancement) was noticed; however, this trend wasn't straightforward for foams with

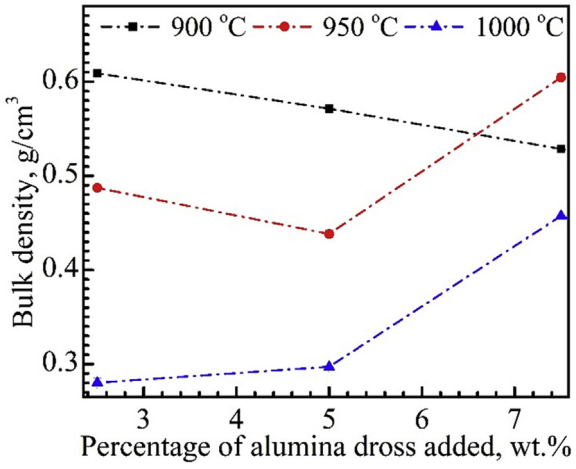

Fig. 7 – Evolution of bulk density with sintering temperature and aluminium dross content.

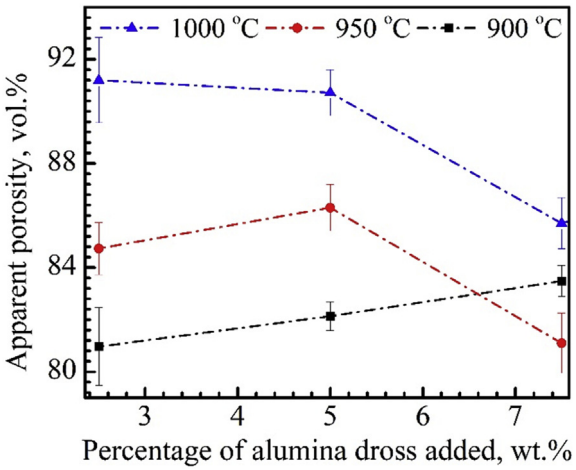

Fig. 8 – Evolution of apparent porosity with sintering temperature and aluminium dross content.

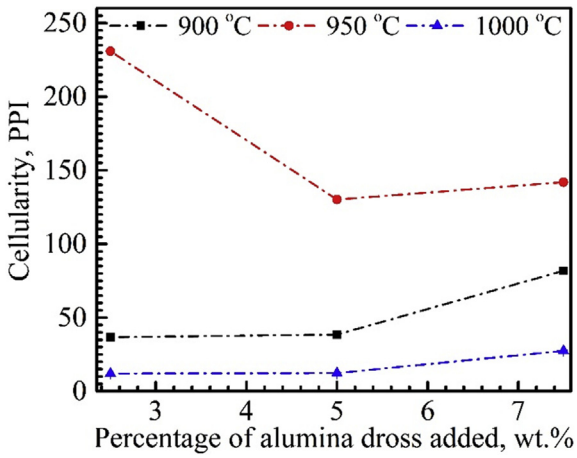

Fig. 9 – Exact cellularity variation with sintering temperature and aluminium dross content.

compositions containing <5.0 wt.% aluminium dross, proposing that these compositions were less susceptible to the temperature variation compared to compositions of lower foaming agent contents. These results are highly compatible with those obtained in reference [12] for glass foams produced from sodium-calcium silicate glass cullet, fly-ash, and SiC foaming agent. Apparently, at 950 °C, density decreased with increasing aluminium dross from 2.5 to 5 wt.% and then increased at higher dross content (<5 wt.%), featuring a V-shaped trend. The most efficient foaming effect at 950 °C was registered for samples containing 5 wt.% of aluminium dross. Such sample "GF5-950" has expanded to around 5 times compared to the green body, registering 86 vol.% porosity, 0.43 g/cm^3 bulk density, 132 PPI cellularity, and 528 ± 200 mean pore size. The decrease in apparent porosity beyond 5 wt.% dross at 950 °C was attributed to the high content of aluminium dross, generation of more gas bubbles, breakdown of the struts, and collapse of the structure. With increasing the sintering temperature up to 1000 °C, the specimens revealed a low-expansion due to the deformation and collapse of the foam structure occurred by the significant reduction in glass viscosity. Following that, the average cellularity of the glasses foamed at 1000 °C decreased significantly to (17 ± 5) and the mean pore size increased considerably to (1241–6594 μm). Based on the results of densification parameters, the best sintering temperature was 950 °C, and the optimal foaming contents were between 2.5 and 5 vol.%. Densification parameters are translations for what happened in the microstructure of the produced foams during sintering. Further, study of the densification parameters of the produced glass foams indicated the high compatibility between the density and porosity values; therefore, it is possible to state that there is a strong relationship between the bulk density and porosity of the resulting glass foams.

3.4. *Cold crushing strength (CCS)*

The CCS values of the resulting foamed specimens were in good correlation with their bulk density values (Fig. 10). The foamed specimens at 900 °C demonstrated the highest CCS values at the expense of their elevated densities. The glass foams sintered at 900 °C had compressive strength values between 6 and 12 MPa, while the CCS values decreased to 4–6 MPa and 1–4 MPa at 950 and 1000 °C. Such decrease in the CCS values corresponds to the porosity enhancement and density decline at higher sintering temperatures since the compressive strength of porous ceramics is basically dependent on the ceramic particles around pores (effective load-bearing struts) which decrease with the increase in porosity at higher sintering temperatures [32,33]. These findings are in agreement with the reported data in references [15,34]. The maximum CCS value was obtained at 900 °C for GF5 containing 5 wt.% aluminium dross due to its low porosity (~82 vol.%), smaller cell size (160 ± 60 μm), and high density (0.57 g/cm^3) together with crystallization of reinforcing crystalline phases (diopside and cristobalite) in its struts [12]. The obtained properties for the waste-derived foams synthesized in this work compare well with those displayed by commercially available glass foams in terms of bulk density (0.28–0.6 g/cm^3), apparent porosity (81–91 vol.%), and compressive strength (1–12 MPa) [10].

3.5. *Thermal characteristics*

Depending on foaming agent content as well as foaming temperature, thermal conductivity, thermal diffusivity, and specific heat capacity of the resulting glass foams ranged between 0.11 and 0.21 W/m-K, 0.4788–1.258 mm^2/s, and 0.09241–0.4482 MJ/m^{3}K, respectively. These values are comparable to those obtained for the foam materials synthesized from the soda-lime glass waste and AlN pore-forming agent [15]. The thermal conductivity of glass foams had an inverse proportion with porosity as well as aperture size and homogeneity [35]. This means that the thermal insulation of the glass foams is improved with the increase in porosity and aperture size provided that the pores are uniformly distributed and orderly arranged since the less evenly distributed pores in the glass foam, the smaller the thermal resistance and, consequently, the worse the thermal insulation. Based on the physical parameters of the fabricated foams (porosity,

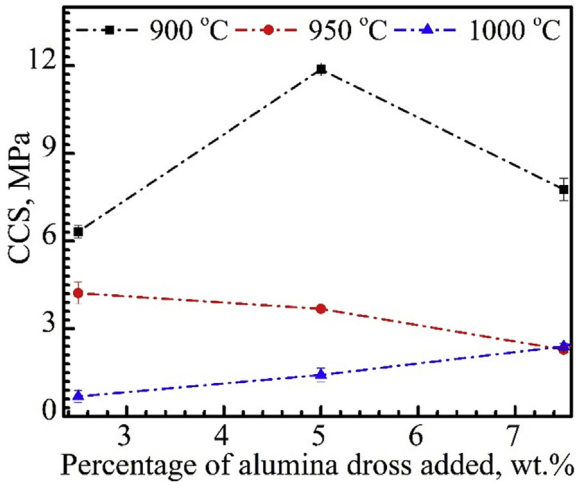

Fig. 10 – Cold crushing strength variation with sintering temperature and aluminium dross content.

Table 4 – Thermal conductivity, thermal diffusivity and specific heat capacity of the glass foams prepared at 900–1000 °C.

Sample ID	Thermal conductivity W/mK	Thermal diffusivity mm^2/s	Specific heat MJ/m^3K	Cellularity Exact PPI
GF2.5@ 900 °C	0.1377	1.258	0.1095	231
GF5@ 900 °C	0.2108	0.4974	0.4239	130
GF7.5@ 900 °C	0.1152	1.246	0.09241	142
GF2.5@ 950 °C	0.1744	0.5063	0.3445	37
GF5@ 950 °C	0.1735	0.4998	0.3471	38
GF7.5@ 950 °C	0.2146	0.4788	0.4482	82
GF2.5@ 1000 °C	0.1432	0.6036	0.2372	12
GF5@ 1000 °C	0.1414	0.5811	0.2433	12
GF7.5@ 1000 °C	0.2172	0.5552	0.3912	27

aperture size and homogeneity), variation of the thermal parameters (thermal conductivity, thermal resistivity, and heat capacity) with the sintering temperature and the amount of aluminium dross were given in Table 4.

4. Conclusion

High-quality glass foams have been successfully prepared from soda-lime glass waste together with aluminium dross as a pore-forming agent at 900–1000 °C for 30 min. The physical, mechanical, and thermal properties of the foamed specimens were duly studied. The experimental results are set out below:

1. The foam samples had a 3-D cellular structure with closed pores of elliptical, pentagonal, and hexagonal geometries
2. Despite their containment of traces of partially crystalline diopside and cristobalite phases, the resultant foamed materials were found to be amorphous in nature
3. The glass foam specimen "GF5-950" containing 5 wt.% aluminium dross and sintered at 950 °C was chosen as the best foamed sample in this work where it has expanded to around 5 times compared to the green body, registering 86 vol.% porosity, 0.43 g/cm^3 bulk density, 132 PPI cellularity, 528 ± 200 mean pore size, 0.17 W/mK thermal conductivity, and ~4 MPa CCS
4. The physico-mechanical and thermal properties achieved by the specimen "GF5-950" are consistent with the requirements of the international standard for commercial glass foams, revealing its strong-susceptibility to be utilized for potential applications in sustainable buildings and energy efficiency in industry as lining or lightweight packing material

Declaration of Competing Interest

The authors declare that they have no known competing financial interests or personal relationships that could have appeared to influence the work reported in this paper.

REFERENCES

[1] Vieitez ER, Eder P, Villanueva A, Saveyn H. End-of-waste criteria for glass cullet: technical proposals. 2011. https://doi.org/10.2791/7150.

[2] USEPA. Advancing sustainable materials management: 2015 fact sheet assessing trends in material generation, recycling, composting, combustion with energy recovery and landfilling in the United States. Washington, DC 20460: United States Environ Prot Agency, Off L Emerg Manag; 2018;(July):22.

[3] Harder IJ. Glass recycling – current market trends - recovery. Recovery; 2018.

[4] US EPA. Textiles: material-specific data | facts and figures about materials, waste and recycling | US EPA. US EPA; 2018. p. 1.

[5] Ji R, Zhang Z, He Y, Liu L, Wang X. Synthesis, characterization and modeling of new building insulation material using ceramic polishing waste residue. Construct Build Mater 2015;85:119–26. https://doi.org/10.1016/j.conbuildmat.2015.03.089.

[6] Bernardo E, Cedro R, Florean M, Hreglich S. Reutilization and stabilization of wastes by the production of glass foams. Ceram Int 2007;33(6):963–8. https://doi.org/10.1016/j.ceramint.2006.02.010.

[7] Arcaro S, De Oliveira Maia BG, Souza MT, Cesconeto FR, Granados L, De Oliveira APN. Thermal insulating foams produced from glass waste and banana leaves. Mater Res 2016;19(5):1064–9. https://doi.org/10.1590/1980-5373-MR-2015-0539.

[8] AG Fedorov LP. Glass foams: formation, transport properties, and heat, mass, and radiation transfer. J Non-Cryst Solids 2002;311(2):154–73.

[9] Bernardo E, Albertini F. Glass foams from dismantled cathode ray tubes. Ceram Int 2006;32(6):603–8. https://doi.org/10.1016/j.ceramint.2005.04.019.

[10] Scheffler M, Colombo P. Cellular ceramics: structure, manufacturing, properties and applications. 2006.

[11] Bai J, Yang X, Xu S, Jing W, Yang J. Preparation of foam glass from waste glass and fly ash. Mater Lett 2014;136:52–4. https://doi.org/10.1016/j.matlet.2014.07.028.

[12] Fernandes HR, Gaddam A, Tulyaganov DU, Ferreira JMF. Design and synthesis of foam glasses from recycled materials. Int J Appl Ceram Technol 2020;17(1):64–74. https://doi.org/10.1111/ijac.13393.

[13] Chen N, Zhang S, Pan X, Zhou S, Zhao M. Foaming mechanism and optimal process conditions of foamed glass based on thermal analysis. J Porous Mater 2020;27(2):621–6. https://doi.org/10.1007/s10934-020-00864-6.

[14] Ercenk E. The effect of clay on foaming and mechanical properties of glass foam insulating material. J Therm Anal Calorim 2017;127(1):137–46. https://doi.org/10.1007/s10973-016-5582-8.

[15] Ewais EMM, Attia MAA, El-Amir AAM, Elshenway AMH, Fend T. Optimal conditions and significant factors for fabrication of soda lime glass foam from industrial waste using nano AlN. J Alloys Compd 2018;747:408–15. https://doi.org/10.1016/j.jallcom.2018.03.039.

[16] Ramaswamy P, Gomes SA, Ravichander NP. Utilization of aluminum dross: refractories from industrial waste. IOP Conf

Ser Mater Sci Eng 2019;577. https://doi.org/10.1088/1757-899X/577/1/012101.
[17] Feng H, Zhang G, Yang Q, Xun L, Zhen S, Liu D. The investigation of optimizing leaching efficiency of al in secondary aluminum dross via pretreatment operations. Processes 2020;8(10):1–13. https://doi.org/10.3390/pr8101269.
[18] Opeyemi Osoba L, Biodun Owolabi O, Isaac Talabi S, Oluropo Adeosun S, Biu E, Umudim O-E. Review on oxide formation and aluminum recovery mechanism during secondary smelting. J Cast Mater Eng 2018;2(2):45–51. https://doi.org/10.7494/jcme.2018.2.2.45.
[19] Adeosun SO, Akpan EI, Dada MO. Refractory characteristics of aluminum dross-kaolin composite. JOM (J Occup Med) 2014;66(11):2253–61. https://doi.org/10.1007/s11837-014-1179-5.
[20] Betke U, Lieb A, Scheffler F, Scheffler M. Manufacturing of reticulated open-cellular aluminum nitride ceramic foams from aqueous AlN suspensions. Adv Eng Mater 2017;19(3). https://doi.org/10.1002/adem.201600660.
[21] Shi H, Feng K qin, Wang H bo, Chen C hong, Zhou H ling. Influence of aluminium nitride as a foaming agent on the preparation of foam glass-ceramics from high-titanium blast furnace slag. Int J Miner Metall Mater 2016;23(5):595–600. https://doi.org/10.1007/s12613-016-1271-7.
[22] Ewais EMM, Khalil NM, Amin MS, Ahmed YMZ, Barakat MA. Utilization of aluminum sludge and aluminum slag (dross) for the manufacture of calcium aluminate cement. Ceram Int 2009;35(8):3381–8. https://doi.org/10.1016/j.ceramint.2009.06.008.
[23] Binner J. Ceramics foams. In: Cell Ceram Struct Manuf Prop Appl. John Wiley & Sons; 2006. p. 31–56. https://doi.org/10.1002/3527606696.ch2a.
[24] Barbosa ARJ, Lopes AAS, Sequeira SIH, Oliveira JP, Davarpanah A, Mohseni F, et al. Effect of processing conditions on the properties of recycled cathode ray tube glass foams. J Porous Mater 2016;23(6):1663–9. https://doi.org/10.1007/s10934-016-0227-7.
[25] Sasmal N, Garai M, Karmakar B. Preparation and characterization of novel foamed porous glass-ceramics. Mater Char 2015;103:90–100. https://doi.org/10.1016/j.matchar.2015.03.007.
[26] Cesconeto FR, Arcaro S, Maia de BGO, Souza MT, Neto JBR, de Oliveira APN. Materiais celulares vítreos obtidos via colagem de gel de uma emulsão de óleo vegetal. Rev Mater 2016;21(2):385–90. https://doi.org/10.1590/S1517-707620160002.0036.
[27] Santos dos PAM, Priebbnow AV, Arcaro S, Silva da RM, Lopez DAR, Rodriguez ADAL. Sustainable glass foams produced from glass bottles and tobacco residue. Mater Res 2018;22(1). https://doi.org/10.1590/1980-5373-mr-2018-0452.
[28] Ewais EMM, Ahmed YMZ, El-Amir AAM, El-Didamony H. Cement kiln dust/rice husk ash as a low temperature route for wollastonite processing. Epa - J Silic Based Compos Mater. 2014;66(3):69–80. https://doi.org/10.14382/epitoanyag-jsbcm.2014.14.
[29] Kumagai S, Sasaki J. Carbon/silica composite fabricated from rice husk by means of binderless hot-pressing. Bioresour Technol 2009;100(13):3308–15. https://doi.org/10.1016/j.biortech.2009.02.001.
[30] Deubener J, Brueckner R, Hessenkemper H. Nucleation and crystallization kinetics on float glass surfaces. Glastechnische Ber 1992;65(9):256–66.
[31] Zanotto ED. Surface crystallization kinetics in soda-lime-silica glasses. J Non-Cryst Solids 1991;129(1–3):183–90. https://doi.org/10.1016/0022-3093(91)90094-M.
[32] Guo H, Ye F, Li W, Song X, Xie G. Preparation and characterization of foamed microporous mullite ceramics based on kyanite. Ceram Int 2015;41(10):14645–51. https://doi.org/10.1016/j.ceramint.2015.07.186.
[33] Chen X, Wu S, Zhou J. Influence of porosity on compressive and tensile strength of cement mortar. Construct Build Mater 2013;40:869–74. https://doi.org/10.1016/j.conbuildmat.2012.11.072.
[34] Tulyaganov DU, Fernandes HR, Agathopoulos S, Ferreira JMF. Preparation and characterization of high compressive strength foams from sheet glass. J Porous Mater 2006;13(2):133–9. https://doi.org/10.1007/s10934-006-7014-9.
[35] Qin Z, Li G, Tian Y, Ma Y, Shen P. Numerical simulation of thermal conductivity of foam glass based on the steady-state method. Materials 2018;12(1). https://doi.org/10.3390/ma12010054.